The Journal of Physiology

Integrin-associated ILK and PINCH1 protein content are reduced in skeletal muscle of maintenance haemodialysis patients

Fulvia Draicchio[1], Stephan van Vliet[2], Oana Ancu[1], Scott A. Paluska[4], Kenneth R. Wilund[2,3], Monika Mickute[6], Thozhukat Sathyapalan[7], Derek Renshaw[8], Peter Watt[9], Lykke Sylow[5], Nicholas A. Burd[2,3] and Richard WA Mackenzie[1]

[1]*Department of Life Sciences, Sport and Exercise Science Research Center, University of Roehampton, London, UK*
[2]*Department of Kinesiology and Community Health, University of Illinois at Urbana-Champaign, Urbana, IL, USA*
[3]*Division of Nutritional Sciences, University of Illinois at Urbana-Champaign, Urbana, IL, USA*
[4]*Department of Family Medicine, University of Illinois at Urbana-Champaign, Urbana, IL, USA*
[5]*Department of Nutrition, Exercise and Sport, August Krogh Bygningen, University of Copenhagen, Denmark*
[6]*Leicester Diabetes Center, Leicester General Hospital, Leicester, UK*
[7]*University of Hull/Hull and East Yorkshire Hospitals NHS Trust, Hull, UK*
[8]*Centre for Sport, Exercise and Life Sciences, Coventry University, Coventry, UK*
[9]*Sport and Exercise Science and Sports Medicine research and enterprise group, Welkin Laboratories, University of Brighton, Eastbourne, UK*

Edited by: Kim Barrett & Javier Gonzalez

Key points

- Patients with renal failure undergoing maintenance haemodialysis are associated with insulin resistance and protein metabolism dysfunction.
- Novel research suggests that disruption to the transmembrane protein linkage between the cytoskeleton and the extracellular matrix in skeletal muscle may contribute to reduced amino acid metabolism and insulin resistance in haemodialysis.
- ILK, PINCH1 and pFAK^{Tyr397} were significantly decreased in haemodialysis compared to controls, whereas Rac1 and Akt2 showed no different between groups.
- Rac1 deletion in the Rac1 knockout model did not alter the expression of integrin-associated proteins.
- Phenylalanine kinetics were reduced in the haemodialysis group at 30 and 60 min post meal ingestion compared to controls; both groups showed similar levels of insulin sensitivity and β-cell function.
- Key proteins in the integrin–cytoskeleton linkage are reduced in haemodialysis patients, suggesting for the first time that integrin-associated proteins dysfunction may contribute to reduced phenylalanine flux without affecting insulin resistance in haemodialysis patients.

Dr Draicchio has a background in Biotechnology before moving into the research theme of Human Metabolism and metabolic disorders of type 2 diabetes and chronic kidney disease in the Laboratory of Dr Richard Mackenzie in collaboration with Dr Nick Burd. Her research suggests that disruption to the transmembrane protein linkage between the cytoskeleton and the extracellular matrix in skeletal muscle may contribute to reduced amino acid metabolism and insulin resistance in hemodialysis. **Richard W.A. Mackenzie** is a Reader in Insulin Resistance and Metabolism at the University of Roehampton (London). With over 10 years' experience in investigating the mechanisms that govern contraction- and insulin-stimulated glucose transport in skeletal muscle, he has a particular interest in the role of inositol hexakisphosphate (IP6) kinase 1 (IP6K1) in the inhibition Akt/PKB and reduced insulin signalling in skeletal muscle. His research focus requires molecular and whole-body approaches to investigate the disease processes in human metabolism and type 2 diabetes.

DOI: 10.1113/JP280441

Abstract Muscle atrophy, insulin resistance and reduced muscle phosphoinositide 3-kinase-Akt signalling are common characteristics of patients undergoing maintenance haemodialysis (MHD). Disruption to the transmembrane protein linkage between the cytoskeleton and the extracellular matrix in skeletal muscle may contribute to reduced amino acid metabolism and insulin resistance in MHD patients. Eight MHD patients (age: 56 ± 5 years: body mass index: 32 ± 2 kg m^{-2}) and non-diseased controls (age: 50 ± 2 years: body mass index: 31 ± 1 kg m^{-2}) received primed continuous L-[*ring*-$^2H_5$]phenylalanine before consuming a mixed meal. Phenylalanine metabolism was determined using two-compartment modelling. Muscle biopsies were collected prior to the meal and at 300 min postprandially. In a separate experiment, skeletal muscle tissue from muscle-specific Rac1 knockout (Rac1 mKO) was harvested to investigate whether Rac1 depletion disrupted the cytoskeleton-integrin linkage, allowing for cross-model examination of proteins of interest. ILK, PINCH1 and $pFAK^{Tyr397}$ were significantly lower in MHD ($P < 0.01$). Rac1 and Akt showed no difference between groups for the human trial. Rac1 deletion in the Rac1 mKO model did not alter the expression of integrin-associated proteins. Phenylalanine rates of appearance and disappearance, as well as metabolic clearance rates, were lower in the MHD group at 30 and 60 min post meal ingestion compared to controls ($P < 0.05$). Both groups showed similar levels of insulin sensitivity and β-cell function. Key proteins in the integrin–cytoskeleton linkage are reduced in MHD patients, suggesting for the first time that integrin-associated proteins dysfunction may contribute to reduced phenylalanine flux without affecting insulin resistance in haemodialysis patients.

(Received 3 July 2020; accepted after revision 9 September 2020; first published online 24 September 2020)
Corresponding author R. Mackenzie: Department of Life Sciences, Sport and Exercise Science Research Centre, Whitelands College, University of Roehampton, 1076 Parkstead House, London SW15 4JD, UK.
Email: richard.mackenzie@roehampton.ac.uk

Introduction

Patients with renal failure undergoing maintenance haemodialysis (MHD) demonstrate several metabolic and phenotypic alterations including muscle wasting (Workeneh & Mitch, 2010; van Vliet *et al.* 2018) as a result of increased degradation of muscle proteins through activation of the ubiquitin-proteasome system (Workeneh & Mitch, 2010). Decreased muscle mass results in decreased motor function and glucose storage capacity (Johansen *et al.* 2003). Using the 'gold standard' euglycaemic-hyperinsulinemic clamp, DeFronzo *et al.* (1981) showed that patients with renal failure demonstrated insulin resistance, a finding that is supported elsewhere (Kobayashi *et al.* 2005; Bailey *et al.* 2006; Semenkovich, 2006; Turcotte & Fisher, 2008; Thomas *et al.* 2015).

Glucose transport into skeletal muscle is known to occur via two distinct pathways: (i) insulin-mediated GLUT4 translocation, partly requiring functional IRS-1-Akt/AS160 signalling (Deshmukh, 2016), and (ii) contraction-stimulated GLUT4 movement via Ca^{+2}-dependent AMPK/AS160 signalling (Wright *et al.* 2005; Kramer *et al.* 2006; Mackenzie & Elliott, 2014; Sylow *et al.* 2017). Of note, it is widely accepted that it is the first pathway that is defective in insulin resistant skeletal muscle. More recently, a third pathway that facilities glucose transport has been identified, termed the tension-mediated pathway (Chambers *et al.* 2009; Jensen *et al.* 2014; Sylow *et al.* 2015). It is hypothesized that this latter pathway requires a structurally stable linkage between the extracellular matrix and the actin–cytoskeleton to encourage normal nutrient uptake.

The dystroglycan complex and integrins are major surface receptors of the extracellular matrix (ECM) in skeletal muscles (Von der Mark *et al.* 1991; Hynes, 2002; Postel *et al.* 2008; Williams *et al.* 2015). Integrins are transmembrane proteins formed by α and β subunits, which mediate interactions between the ECM and the cytoplasmic cytoskeleton (Postel *et al.* 2008), and they are responsible for transducing signals across the membrane to the intracellular integrin-binding proteins (Williams *et al.* 2015; Kang *et al.* 2016). Although the role of integrins in ECM and muscle cell integrity has been extensively characterized (Legate & Fässler, 2009; Wickström *et al.* 2010), little is known about the function of the integrin-binding intracellular complexes in both mechanical stability (Postel *et al.* 2008; Wickström *et al.* 2010) and normal nutrient metabolism in skeletal muscle. Once activated, the integrin complex stimulates downstream targets implicated in both insulin-like growth factor and insulin receptor substrate signalling, including integrin-linked kinase (ILK), focal adhesion kinase (FAK), serine/threonine-specific protein kinase (Akt), Rho GTPase Rac1 and glycogen synthase kinase 3β

(GSK-3β) (Williams *et al.* 2015). Thus, integrin and its associated target kinases appear to be implicated in muscle protein synthesis (Byun *et al.* 2012; Clemente *et al.* 2012), insulin-mediated glucose uptake (Huang *et al.* 2006; Bisht *et al.* 2007; Bisht & Dey, 2008) and cytoskeletal stabilization (Williams *et al.* 2015).

Muscle atrophy, a recognized characteristic of MHD (van Vliet *et al.* 2018), has been linked with reduced muscle integrin-associated protein content (Pattison *et al.* 2004; Postel *et al.* 2008; Wang *et al.* 2008; Peter *et al.* 2011). In addition, reduced integrin-associated protein expression is also noted in insulin resistance with decreased Akt phosphorylation, a candidate for reduced insulin-mediated glucose (Urso *et al.* 2006). Given that kidney failure patients display signs of muscle atrophy (Workeneh & Mitch, 2010; van Vliet *et al.* 2018), we hypothesized that MHD patients would demonstrate reduced integrin-associated protein content in skeletal muscle compared to non-MHD individuals. We further hypothesized that the structural and signalling disruption might lead to impaired regulation of protein metabolism and nutrient flux. The present study used two compartment whole-body measures of phenylalanine kinetics and surrogate measures of insulin resistance to partly test this hypothesis.

Rac1 is a well characterized member of Rho GTPase family and is implicated in cytoskeletal reorganization, transcriptional regulation, cell migration and nutrient uptake (Burridge & Wennerberg, 2004; Ueda *et al.* 2008). Rac1 is known to promote GLUT4 translocation and glucose uptake via mechanisms requiring actin remodelling in skeletal muscle (Török *et al.* 2004; JeBailey *et al.* 2007; Sylow *et al.* 2013*b*). Thus, proteins involved in vesicle trafficking may only operate fully in the presence of a functional cytoskeleton (Ueda *et al.* 2008). The ILK PINCH parvin (IPP) complex functions at one of the early steps of the integrin signalling cascade (Wu, 1999; Stanchi *et al.* 2009). The pseudokinase integrin-linked kinase ILK recruits downstream targets implicated in insulin-mediated glucose uptake and links integrins to the actin cytoskeleton (Gheyara *et al.* 2007); among its downstream targets, there are PDK1 and GSK-3β (through PINCH1), as well as α-actinin and Rac1 (through parvin) (Williams *et al.* 2015). ILK directly interacts with the β-integrin subunits and is stimulated by both integrin activation and growth factors and appears to act as an upstream regulator of Akt (Wu & Dedhar, 2001; Tang *et al.* 2007). Therefore, this integrin signalling pathway is suggested to facilitate glucose uptake via both insulin-dependent and independent mechanisms in a cross-sarcolemma fashion.

Accordingly, in the present study, we probed skeletal muscle from insulin resistant, but otherwise healthy controls, and made comparisons with MHD patients in both a fasted and postprandial state for integrin-associated protein signalling. Using an established muscle-specific Rac1 knockout rodent model (Sylow *et al.* 2013*a*; Raun *et al.* 2018), a secondary aim was to investigate the potential linkage between actin cytoskeleton and integrin-associated signalling.

Methods

Ethical approval

Ethics for human experiments was approved by the local Ethics Board (University of Illinois at Urbana-Champaign) and met all conditions outlined in the seventh revision of the *Declaration of Helsinki* for use of human volunteers (Clinical Trial Registration Number: NCT03478722).

All experiments regarding the mouse models were approved by the Danish Animal Experimental Inspectorate (License: 2016-15-0201-0 1043).

Human experiment

Eight MHD patients [mean ± SEM age 56 ± 5 years, male sex = 6 (75%), body mass index = 32 ± 2 kg m^{-2}, body fat = 31 ± 3%, homeostatic model assessment of insulin resistance ($HOMA_{IR}$) = 3.9 ± 0.9 and $HOMA_{\beta\text{-cell}}$ = 4.3 ± 1.24] and eight matched insulin resistant controls [age 50 ± 2 years, male sex = 6 (75%), body mass index = 31 ± 1 kg m^{-2}, body fat = 29 ± 2%, $HOMA_{IR}$ = 4.0 ± 0.6 and $HOMA_{\beta\text{-cell}}$ = 4.8 ± 0.65] were recruited for the study. These participants were part of a larger investigation being conducted in our laboratory. [$HOMA_{IR}$; fasting insulin (μU mL^{-1}) × fasting glucose (mmol L^{-1})/22.5] and HOMA of β-cell function [$HOMA_{\beta\text{-Cell}}$; 20 × fasting insulin (μU mL^{-1})/fasting glucose – 3.5 (mmol L^{-1})] were calculated using validated equations (Uwaifo *et al.* 2002). Volunteers received written and verbal details on the experimental design, the study aims and potential risks before providing their written consent. For MHD patients, we requested physician clearance from their nephrologist to further that ensure it was safe for the patient to participate in the study.

A full description of the pre-screening and experimental procedures is provided elsewhere (van Vliet *et al.* 2018). The MHD patients analysed in the present study have been in dialysis treatment for ∼5 years and their current nutritional status comprised ingestion of protein-rich meals to achieve the recommended protein intakes (set at 1.2 g kg^{-1} body weight day^{-1}) to limit muscle protein losses observed in end-stage kidney disease.

MHD patients were studied ∼24 h after a dialysis treatment session (i.e. non-dialysis day). Volunteers ingested an identical meal (320 kcal; 22 g of protein, 43 g of carbohydrates, 7 g of fat) at least 12 h prior to trials and arrived in a fasted state to the laboratory

at 07.00 h. An 18-gauge cannula was positioned into a dorsal hand vein to allow frequent sampling of arterialized blood (every 30–60 min) with a thermoregulated hot box (∼65°C). A second 18-gauge cannula was placed into an antecubital vein for the primed constant infusion of L-[*ring*-$^2H_5$]phenylalanine (prime; 2.0 μmol kg^{-1} free fat mass, infusion rate; 0.05 μmol kg^{-1} free fat mass min^{-1}). A baseline blood sample was collected at $t = -180$ min immediately prior to the start of the infusion protocol. Muscle biopsies were collected at $t = -120$ and -0 min of the infusion, reflecting a post-absorptive state.

Subsequently, volunteer ingested a mixed meal (546 kcal; 20 g of protein, 59 g of carbohydrates, 26 g of fat), the completion of which marked the start of the postprandial phase ($t = 0$ min). An additional muscle biopsy was collected at 300 min. Biopsies were sampled from the middle region of the vastus lateralis (15 cm above the patella) with a Bergström needle modified for suction under local anaesthesia (2% lidocaine) (van Vliet *et al.* 2018). The post-absorptive muscle biopsies were sampled from the same incision with the needle pointed in the distal and proximal directions, respectively (van Vliet *et al.* 2018). Muscle samples were immediately frozen in liquid nitrogen and stored at −80°C until subsequent analysis. Blood samples were centrifuged at 3000 ***g*** for 10 min at 4°C and plasma was stored at –80°C for subsequent analysis.

Mouse models

Considering the importance of an intact cytoskeleton for normal glucose uptake in skeletal muscles, we aimed to investigate the potential role of the major actin regulators, Rac1, in the integrin signalling pathway. Thus, nine muscle specific tetracycline-inducible knockout (mKO) mice and seven control mice were analysed in the present study. A full description of the Rac1 muscle-specific tetracycline-inducible knockout (mKO) mouse model used in this experiment is provided elsewhere (*Sylow et al. 2013b*, 2013*a*). Skeletal muscle from Rac1 mKO mice were analysed when the mice were 31–33 weeks of age. Rac1 mKO was induced at 12–16 weeks of age by adding doxycycline (a tetracycline analogue) in the drinking water (1 g L^{-1}; Sigma Aldrich, Copenhagen, Denmark) for 3 weeks to deplete Rac1 specifically in skeletal muscle (PMID: 29 749 029). This treatment was repeated at week 10 of the intervention period to ensure continuous Rac1 knockout throughout the entire intervention period. An 18-week diet intervention was started at 14–18 weeks of age and mice received either a standard rodent chow diet (Altromin no. 1324; Brogaarden, Horsholm, Denmark) or a 60% high-fat diet (HFD) (no. D12492; Brogaarden) and water *ad lib.* Body weight was assessed every week. In the present study, we investigated skeletal muscles of chow-fed mice. All animals were maintained under a 12:12 h light/dark photocycle, and group housed at 20–21°C. For muscle tissue sampling, mice were fasted for 3–5 h from 07.00 h and anaesthetized (I.P. injection of 7.5/9.5 mg (chow/HFD) pentobarbital sodium 100 g^{-1} body weight). After 25 min, skeletal muscle was excised and quickly frozen in liquid nitrogen and stored at –80°C until processing.

Immunoblotting

Relative total muscle protein content and phosphorylation levels of relevant proteins were determined by standard immunoblotting techniques loading equal amounts of protein. The primary antibodies used were anti-Integrin linked ILK antibody (ab227154; Abcam, Cambridge, MA, USA), anti-PINCH1 antibody [EP1943Y] (ab76112; Abcam), α-parvin (D7F9) XP Rabbit mAb (8190S; Cell Signaling Technology, Beverly, MA, USA) (37), pFAK^{Tyr397} (D20B1) Rabbit mAb (8556S; Cell Signaling Technology) (Tuguzbaeva *et al.* 2019), anti-total FAK (ab40794; Abcam) (Bian *et al.* 2019), anti-Rac1 (ARC03; Cytoskeleton Inc., Denver, CO, USA) (Raun *et al.* 2018), anti-total Akt2 (no. 3063; Cell Signaling Technology) (Raun *et al.* 2018), pAkt^{S473} (no. 9271; Cell Signaling Technology) (Karusheva *et al.* 2019), pAkt^{T308} (no. 9275; Cell Signaling Technology) (Raun *et al.* 2018), anti-IP6K1 antibody (ab129595; Abcam) and anti-dystrophin (ab15277; Abcam) (Jelinkova *et al.* 2019).

Polyvinylidene difluoride membranes (Immobilon TransferMembrane; Millipore, Burlington, MA, USA) were blocked in Tris-buffered saline-Tween 20 containing 2% skimmed milk or 5% BSA protein for 30–60 min at room temperature. Membranes were incubated with primary antibodies overnight at 4°C, followed by incubation with rabbit or mouse peroxidase-conjugated secondary antibody for 30 min at room temperature. Coomassie brilliant blue staining was used as a loading control (Welinder & Ekblad, 2011). Bands were visualized using the ChemiDoc MP Imaging System (Bio-Rad, Hercules, CA, USA). Raw data for all the above protein analysed are openly available via figshare: https://doi.org/10.6084/m9.figshare.12886943.

Blood analysis

Blood metabolites were determined using a point-of-care chemistry analyser (Piccolo Xpress Chemistry Analyzer; Abaxis, Union City, CA, USA). Plasma insulin concentrations were determined using a commercially available enzyme-linked immunosorbent assays (Alpco Diagnostics, Salem, NH, USA). Plasma phenylalanine concentrations (unlabelled) and phenylalanine enrichments (labelled) were determined by gas chromatography-mass spectrometry analysis (Agilent 7890A GC/5975C; MSD, Little Falls, DE, USA)

as described previously (van Vliet *et al.* 2016). Briefly, plasma samples were prepared for amino acid analysis using a mixture of isopropanol:acetonitrile:water (3:3:2, v/v) and centrifuged at 20 000 ***g*** for 10 min at 4°C. Subsequently, the supernatant was dried, and the amino acids converted into tert-butyldimethylsilyl derivatives prior to gas chromatography-mass spectrometry analysis. L-[*ring*-$^2H_5$]phenylalanine, *m/z* 336 (*m*+0) and 341 (*m*+5) were monitored for unlabelled and labelled phenylalanine, respectively.

Data modelling

Plasma insulin and endogenous glucose concentrations were used to model the measures of insulin sensitivity (ISI) (Matsuda index) (Matsuda & Defronzo, 1999): acute insulin response to glucose (AIR_g), second phase insulin response ($\Delta I_{60–120}/\Delta G_{60–120}$) (Lorenzo *et al.* 2013) and disposition index ($DI = S_I \times AIR_g$) (Utzschneider *et al.* 2009).

Whole body phenylalanine rate of disappearance (R_d), rate of appearance (R_a) and metabolic clearance rates (MCR values) were calculated as described previously (Bergman *et al.* 1989; Gastaldelli *et al.* 1999; Barclay *et al.* 2020). Raw data for insulin and phenylalanine metabolism are openly available via figshare: https://doi.org/10.6084/m9.figshare.12886943.

Statistical analysis

R software (R Foundation for Statistical Computing, Viena, Austria) and the *Lme4* package (Bates *et al.* 2015) were used to perform linear mixed effects analyses of the relationship between insulin, phenylalanine or protein values, and time and condition (controls and MHD). Condition interacting with time was entered as a fixed effect into the model, whereas the main effects of subjects and time were considered as the random effects. If the null hypothesis was rejected, *post hoc* tests were performed to determine which groups differed from each other. $P < 0.05$ was considered statistically significant.

Results

ISI

$HOMA_{IR}$ and $HOMA_{\beta\text{-Cell}}$ ($P > 0.05$) were comparable between groups, suggesting no difference metabolic dysfunction between MHD and non-MHD individuals (data not shown). Estimations of ISI and β-cell function based on the 59 g of oral carbohydrate load are shown in Fig. 1. These data show that there were no significant differences for ISI ($P = 0.3948$) (Fig. 1*A*). β-cell function was also similar between groups with AIR_g ($P = 0.2006$) (Fig. 1*B*), second phase insulin response to oral glucose ($P = 0.8286$) (Fig. 1*C*) or DI ($P = 0.5605$) (Fig. 1*D*), showing no difference at 2 h after feeding.

Whole-body protein metabolism was estimated using L-[*ring*-$^2H_5$]phenylalanine to allow for the calculations of phenylalanine R_a, R_d and MCR (Fig. 2) from time 0 to 300 min of the postprandial period. The MHD group showed a significant decrease in R_a, ($P = 0.0451$ at 30 min, $P = 0.0131$ at 60 min; $P = 0.0002$ at 90 min and $P = 0.0015$ at 300 min) (Fig. 2*A* and *B*), R_d ($P = 0.0007$ at 30 min, $P = 0.0022$ at 60 min; $P = 0.0003$ at 90 min and $P = 0.00141$ at 300 min) (Fig. 2*C* and *D*) and MCR ($P = 0.0021$ at 30 min; $P = 0.0025$ at 60 min; $P = 0.0001$ at 90 min and $P = 0.0003$ at 300 min) (Fig. 2*E* and *F*) in the 300 min after feeding that, overall, was not apparent for the control group. In the controls, R_a, ($P = 0.9664$ at 30 min; $P = 0.9933$ at 60 min; $P = 0.1129$ at 90 min and $P = 0.2512$ at 300) (Fig. 2*A* and *B*) and R_d ($P = 0.6071$ at 30 min; $P = 0.3175$ at 60 min; $P = 0.1523$ at 90 min and $P = 0.903$ at 300 min) (Fig. 2*C* and *D*) did not show relevant changes after feeding, whereas MCR (Fig. 2*E* and *F*) only showed a decrease at 90 min ($P = 0.0247$) and 300 min ($P = 0.0252$), but not at 30 min ($P = 0.7865$) or 60 min ($P = 0.6762$).There were significantly differences at 30 min for R_d ($P = 0.0476$) and MCR ($P = 0.0345$), but not for R_a ($P = 0.1595$), between groups.

Both R_a ($P = 0.0501$) and R_d ($P = 0.0402$) were significantly different at 60 min, whereas MCR expressed a tendency to be different ($P = 0.0695$). Similar trends between groups were observed at 90 min (R_a, $P = 0.2539$; R_d, $P = 0.4363$; MCR, $P = 0.1637$) and 300 min (R_a, $P = 0.2977$; R_d, $P = 0.415$; MCR, $P = 0.4043$).

Human skeletal muscle analysis

We investigated total and phosphorylated states of proteins implicated in the integrin signalling cascade, as well as those involved in the insulin-dependent pathway in eight MHD patients and eight controls. From the western blot analyses, ILK (Fig. 3*A*) and PINCH1 protein content (Fig. 3*B*), proxy indicators of integrin signalling activity, were significantly reduced in the MHD patients compared to the controls in both the fasted ($P = 0.0133$ and $P = 0.0001$, respectively) and postprandial ($P = 0.0001$ and $P = 0.0001$, respectively) state. $pFAK^{Tyr397}$/tFAK (Fig. 3*D*) was also reduced in MHD; however, statistical analyses revealed a significant decrease in the fasted state ($P = 0.0026$), but not in the postprandial ($P = 0.1164$) state. The actin cytoskeleton regulating protein Rac1 was not different in MHD compared to control ($P = 0.5783$ and $P = 0.3024$ in the fasted and postprandial states, respectively) (Fig. 3*E*). Representative blots are shown in Fig. 3*H*. No difference was noted for either Akt2 ($P = 0.8552$ and $P = 0.2496$ in the fasted and postprandial

states, respectively) (Fig. 4*A*) or IP6K1 ($P = 0.4544$ and $P = 0.2759$ in the fasted and postprandial states, respectively) (Fig. 4*B*) between groups. Representative blots are shown in Fig. 4*C*. Parvin ($P = 0.6778$ fasted and $P = 0.2886$ postprandially) (Fig. 4*C*), total FAK ($P = 0.3963$ fasted and $P = 0.6549$ postprandially) (Fig. 4*E*) and dystrophin ($P = 0.3091$ fasted and $P = 0.437$ postprandially) (Fig. 4*G*) were similar between groups. No bands were detected for phosphorylation targets at Akt^{S473} or Akt^{T308} in control or in MHD skeletal muscles (data not shown). No significant differences were observed in protein content between fasted and postprandial state for ILK ($P = 0.1742$ for MHD and $P = 0.5391$ for controls) (Fig. 3*A*), PINCH1 ($P = 0.5384$ for MHD and $P = 0.2276$ for controls) (Fig. 3*B*), parvin ($P = 0.6804$ for MHD and $P = 0.4003$ for controls) (Fig. 3*C*), $pFAK^{Tyr397}$ ($P = 0.9352$ for MHD and $P = 0.2554$ for controls) (Fig. 3*D*), dystrophin ($P = 0.1533$ for MHD and $P = 0.1324$ for controls, Fig. 3*G*) or IP6K1 ($P = 0.7282$ for MHD and $P = 0.0783$ for controls) (Fig. 4*B*), except for total FAK and Rac1, which resulted significantly decrease post meal ingestion in controls [$P = 0.0342$ (Fig. 3*E*) and $P = 0.033$ (Fig. 3*F*), respectively], but not in the MHD ($P = 0.0551$ and $P = 0.052$, respectively) and total Akt2 that resulted reduced post meal in the MHD group ($P = 0.0051$) (Fig. 4*A*), but not in the controls ($P = 0.0693$).

Rac1 mKO mouse muscle analysis

In a separate experiment, skeletal muscle from nine muscle-specific Rac1 knockout (Rac1 mKO) and seven wild-types was analysed. Rac1 is a well-known regulator of the actin cytoskeleton (JeBailey *et al.* 2007), although it is unknown whether Rac1 regulates the protein expression of the integrin nexus and actin cytoskeleton proteins. Rac1 deletion did not alter the expression of integrin-associated proteins compared to the wild-type in skeletal muscle [ILK, $P = 0.774$ (Fig. 5*A*); PINCH1, $P = 0.0589$ (Fig. 5*B*); parvin, $P = 0.0696$ (Fig. 5*C*); $pFAK^{Tyr397}$, $P = 0.9984$ insulin-stimulated and $P = 0.9116$ not insulin-stimulated, (Fig. 5*D*); total FAK, $P = 0.9784$ (Fig. 5*E*)] confirming the results obtained in the MHD human samples, where Rac1 protein expression was unaltered. Also, $pAkt^{S473}$ ($P = 0.2496$ insulin-stimulated and $P = 0.9974$ not insulin-stimulated) (Fig. 5*G*), $pAkt^{T308}$ ($P = 0.8119$ insulin-stimulated and $P = 0.9986$ not insulin-stimulated) (Fig. 5*H*) and total Akt2 ($P = 0.857$, Fig. 5*I*) levels were not altered by the lack of Rac1 as also reported previously (Raun *et al.* 2018). The activity of both $pAkt^{S473}$ and $pAkt^{T308}$ increased under insulin stimulation within the Rac1 mKO ($P = 0.0551$ and $P = 0.0509$, respectively, Figure 5G and H as well as within the wild type ($P = 0.0022$ and $P = 0.0247$, respectively, Figure 5G and H) compared with saline. $pFAK^{Tyr397}$ activity was unaltered

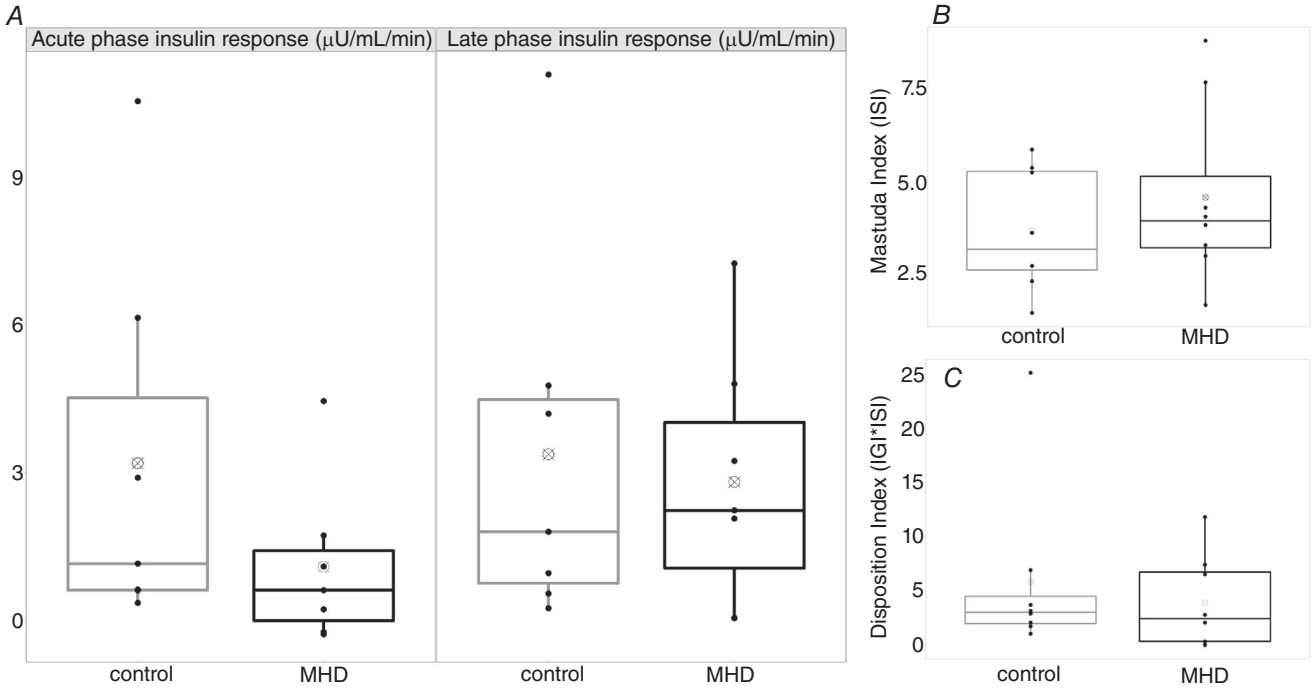

Figure 1. Insulin response to glucose
Acute insulin response to glucose (AIR_g) (left) and second phase insulin response (right) (*A*), Matsuda index (ISI) (*B*) and disposition index (DI) (*C*), after mixed meal feeding in maintenance haemodialysis (MHD, $n = 8$) patients and control ($n = 8$) participants. No statistically significant differences were observed ($P > 0.05$). Quartiles, means and individual data points are shown.

by insulin stimulation within both groups (Rac1 mKO; $P = 0.4904$ and $P = 9127$; WT, Figure 5D), confirming the results observed in the MHD models, where a decrease in pFAK^{Tyr397}, together with ILK or PINCH1 did not alter insulin sensitivity's levels in MHD compared to controls. Furthermore, IP6K1 ($P = 0.3278$) (Fig. 5*F*) and dystrophin ($P = 0.2054$) (Fig. 5*L*) expression was similar in both Rac1 mKO and wild-type. Blots in Fig. 5*M* and *N* were cropped from the same membrane.

Discussion

The present study investigated integrin-associated protein signalling in skeletal muscle of MHD patients. In addition, using a Rac1 KO insulin resistant rodent model, we also examined the potential role that this important actin–cytoskeleton regulatory protein would play in upstream integrin-associated signalling in skeletal muscle. We hypothesized that integrin-associated protein expression would be reduced in both MHD patients

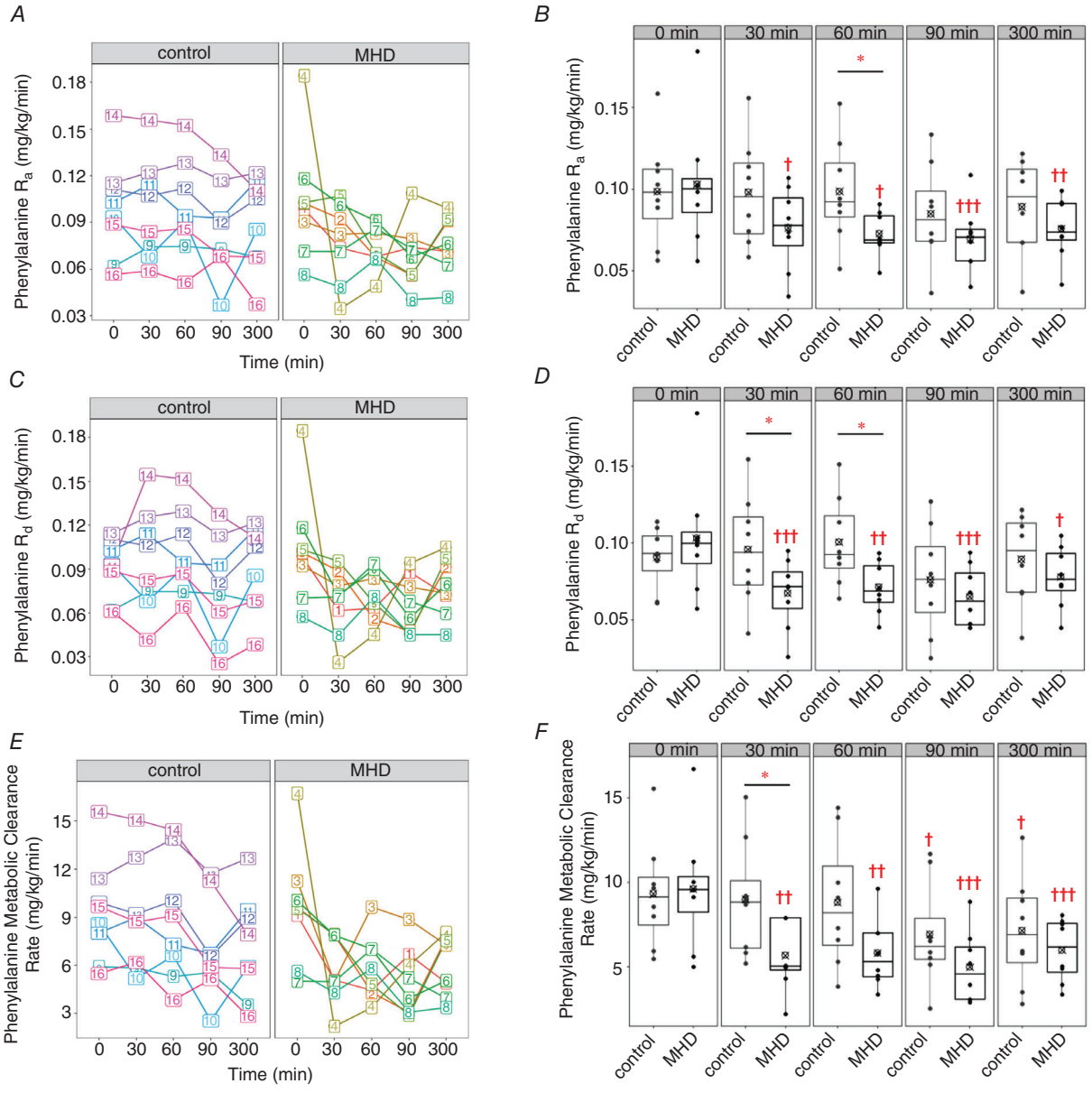

Figure 2. Whole-body phenylalanine kinetics
Whole-body phenylalanine kinetics at baseline and postprandial for both MHD and controls (MHD, $n = 8$ and controls, $n = 8$). Phenylalanine R_a (*A* and *B*), phenylalanine R_d (*C* and *D*) and phenylalanine MCR (*E* and *F*) at baseline, as well as 30, 60, 90 and 300 min post meal ingestion. *A*, *C* and *E*, phenylalanine trend over time of each individual. *B*, *D* and *F*, individual data points, quartiles and means. *Significant difference between MHD and non-MHD ($P < 0.05$). †Significant differences from time 0. *$P < 0.05$, **$P < 0.01$, ***$P < 0.001$. †$P < 0.05$, ††$P < 0.01$, †††$P < 0.001$.

and Rac1 KO rodents. However, it was unclear from the literature whether a loss of the integrin-associated protein structure would facilitate or hinder amino acid metabolism and/or ISI (i.e. nutrient flux) in the MHD patients. Here, we show, for the first time, that phenylalanine flux was reduced in the period immediately post meal ingestion (30 and 60 min) in MHD patients compared to controls. In addition, we also noted a reduction in the integrin-associated protein expression (ILK and PINCH1) for the same comparison.

Evidence suggests that the over development of the ECM structure is linked to increased insulin resistance in mouse models (Kang *et al.* 2011, 2013, 2014; Williams *et al.* 2015) as a result of a proposed increase in the physical barrier to hormonal and nutrient transport across the sarcolemma (Jansson, 2007; Williams *et al.* 2015). In support of this, Williams *et al.* (2015) suggested that ECM protein accumulation within the interstitial space impedes substrate transport as a result of increased diffusion distance. Located directly downstream of the ECM structure,

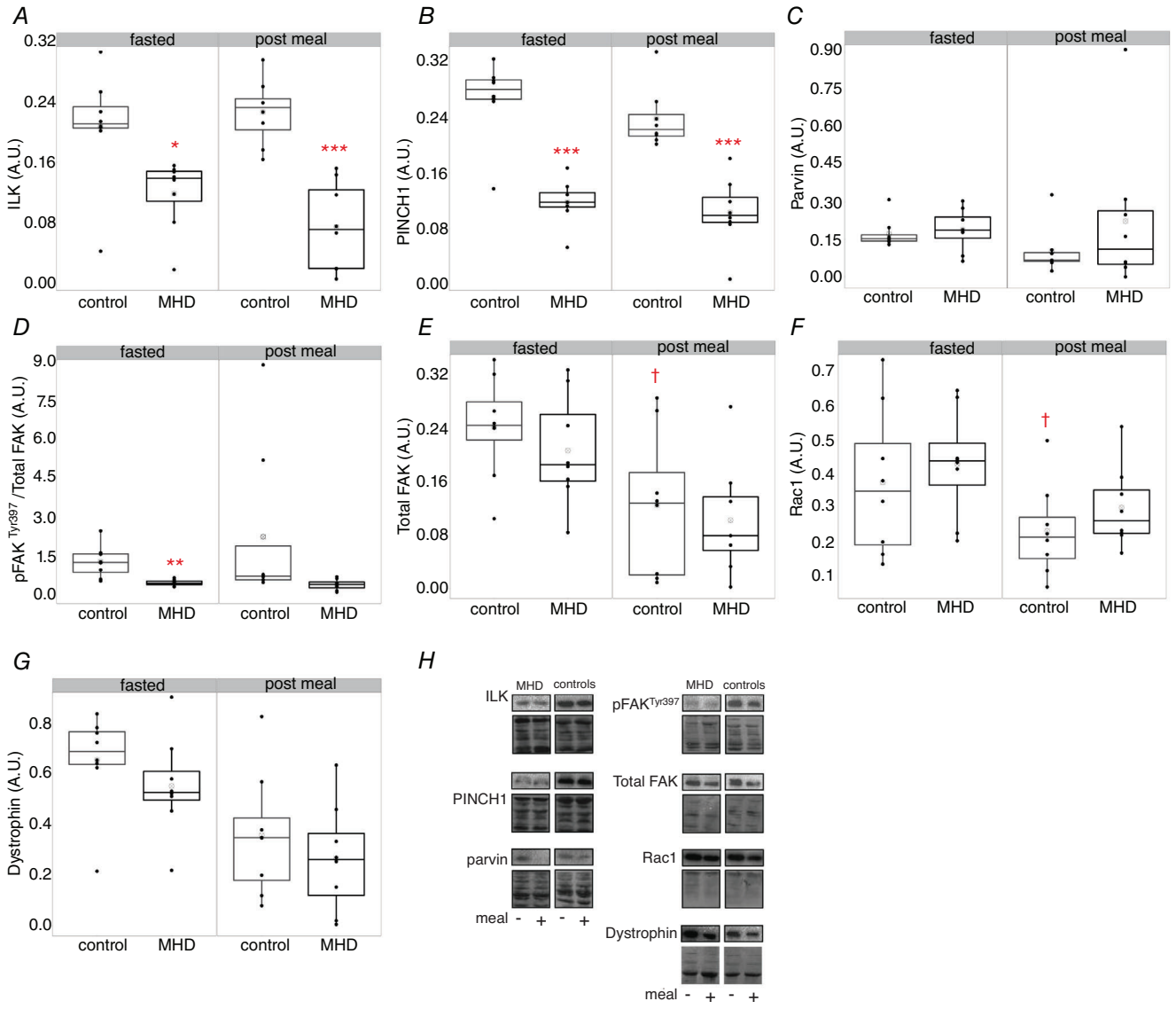

Figure 3. Skeletal muscle protein content in insulin resistant control and MHD patients
Skeletal muscle protein content for targets of interest in insulin resistant control and MHD patients. Content in the fasted state and post meal ingestion (MHD, $n = 8$ and controls, $n = 8$) of ILK (*A*), PINCH1 (*B*), parvin (*C*), pFAK^{Tyr397}/total FAK (*D*), total FAK (*E*), Rac1 (*F*) and dystrophin (*G*). Representative western blots including the corresponding Coomassie brilliant blue staining of the proteins of interest (*H*). *Significant difference between MHD and non-MHD. †Significant differences between fasted and post meal within the same group. *$P < 0.05$, **$P < 0.01$, ***$P < 0.001$. †$P < 0.05$, ††$P < 0.01$, †††$P < 0.001$. Quartiles, means and individual data points are shown.

cytoplasmic integrin-associated proteins appear to have an important role as effectors in integrins signalling in skeletal muscle, providing an essential linkage between the ECM, the sarcolemma and the actin–cytoskeleton (Gheyara *et al.* 2007), therefore contributing to ECM structure stability. Integrin-deficient mice show progressive muscle dystrophy after birth (Mayer *et al.* 1997) as a result of a decreased function of the myotendinous junction (MTJ), which gives structural stability between ECM and the associated myofibrils and their non-contractile structural proteins (Postel *et al.* 2008). The central component of the IPP complex, ILK, is recruited to the MTJ, which requires the presence of the ECM protein laminin, as well as integrin-α7 in the sarcolemma (Postel *et al.* 2008), suggesting the involvement of ILK in ECM stability. In line with our hypothesis, our data showed a reduction in integrin-associated ILK and PINCH1, suggesting that MHD patients may present with reduced stability in the extracellular matrix as a result of dysregulation of integrin-associated protein signalling.

Yet the influence of a reduced integrin-associate protein nexus on nutrient uptake is unclear. The research suggests that the over development of the ECM and its transmembrane associated structures are linked to insulin resistance in mouse models (Kang *et al.* 2011, 2013, 2014; Williams *et al.* 2015). In support of this Williams *et al.* (2015) have shown that ECM protein accumulation within the interstitial space impedes substrate transport. Conversely, Kang *et al.* (2013) demonstrated that a reduction of ECM-associated glycosaminoglycan hyaluronan induced by I.V. injection of PEGylated recombinant hyaluronidase PH-20 led to a dose-dependent increase in glucose infusion rates and glucose clearance in mouse skeletal muscle during a hyperinsulinemic–euglycaemic clamp. Taken together, these data may suggest that an increase in protein content within both the interstitial space and ECM is linked to insulin resistance and reduced nutrient transport, whereas a reduction in the protein content within these compartments may increase nutrient uptake as a result of a reduction in the physical barrier between the ECM and the intracellular compartments. Therefore, we further postulated that a reduction in the integrin-associated nexus and a reduction in ECM structural protein content may result in increased phenylalanine flux and improved glucose handling in MHD patients during the post-absorptive state (Williams *et al.* 2015).

Total phenylalanine rate of appearance (R_a) is a measure of the appearance of dietary protein-derived phenylalanine and that from whole body protein breakdown into circulation (van Vliet *et al.* 2018), whereas phenylalanine R_d and MCR reflect whole-body amino acid clearance and its subsequent utilization and storage to the different tissue compartments within the body (Matthews, 2007; Barclay *et al.* 2020).

In the present study, we show that one-compartment models of the Matsuda index (ISI) and disposition index (DI) were similar between groups, whereas phenylalanine R_a, R_d and MCR rates decreased immediately after time 0 in MHD but not in controls, who maintained a more constant trend over time, suggesting that the haemodialysis group may suffer from decreased skeletal muscle amino acid uptake and utilization in the post-absorptive state. Moreover, phenylalanine R_a, R_d and MCR were also significantly lower in the period immediately after feeding (30 and 60 min) in the MHD group. Taken together, these results suggest that disruptions to the integrin-associate protein nexus may contribute to dysregulation in amino acid metabolism but not ISI (Fig. 1).

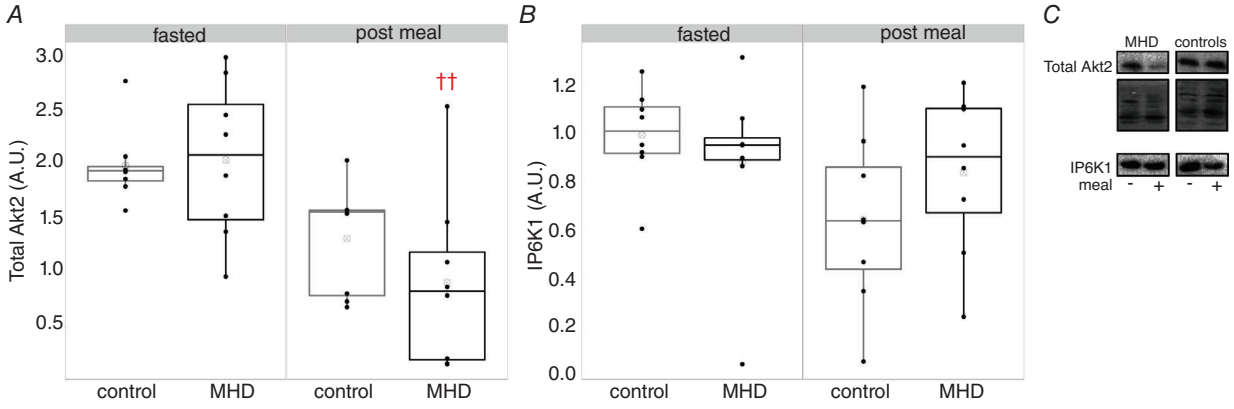

Figure 4. Skeletal muscle protein content for Akt2 and IP6K1
Skeletal muscle protein content for Akt2 (*A*) and IP6K1 (*B*) in the fasted state and post meal ingestion (MHD, $n = 8$ and controls, $n = 8$). Representative western blots of the proteins of interest including the corresponding Coomassie brilliant blue staining, except for IP6K1 (*C*). No significant difference was noted ($P > 0.05$). †Significant differences between fasted and post meal within the same group. †$P < 0.05$, ††$P < 0.01$, †††$P < 0.001$. Quartiles, means and individual data points are shown.

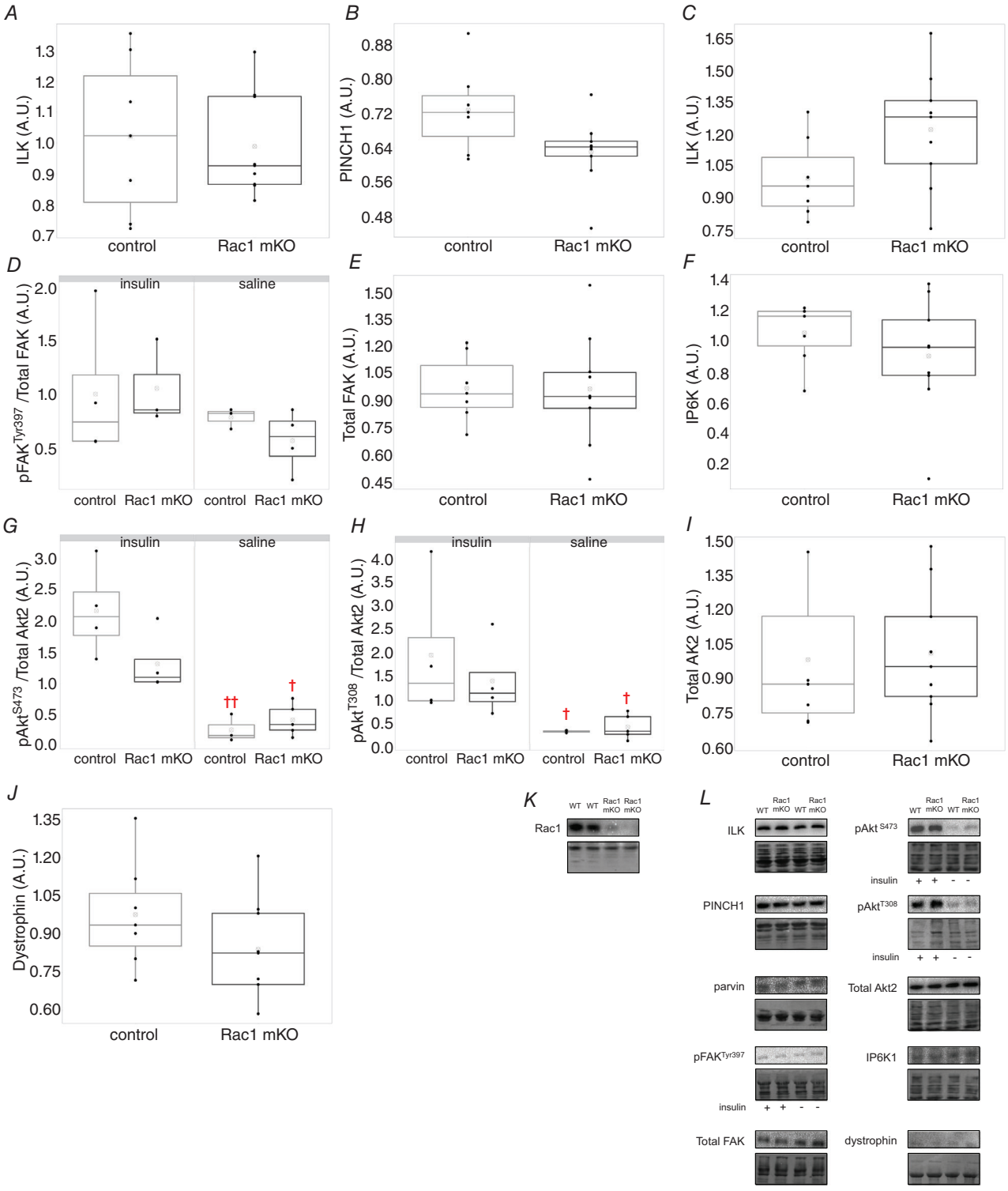

Figure 5. Skeletal muscle protein content of targets of interest in TA muscles
Skeletal muscle protein content of targets of interest in TA muscles of chow-fed WT (n = 7) and Rac1 mKO mice (n = 9). Insulin-stimulated and not insulin-stimulated (saline) samples were considered as separated groups for the phosphorylated proteins. Content of ILK (*A*), PINCH1 (*B*), parvin (*C*), pFAK^{Tyr397}/total FAK (*D*), total FAK (*E*), IP6K1 (*F*), pAkt^{S473}/total Akt2 (*G*), pAkt^{T308}/total Akt2 (*H*), total Akt2 (*I*) and dystrophin (*J*). Representative western blots of Rac1 including the corresponding Coomassie brilliant blue staining, confirming the effectiveness of knockout (*K*). Representative blots including the corresponding Coomassie brilliant blue staining (*L*). Analogous results were obtained in gastrocnemius mouse muscles. No significant difference was noted ($P > 0.05$). † Denotes significant differences between saline and insulin stimulation within the same group. † P<0.05, †† P<0.01, ††† P<0.001.Quartiles, means and individual data points are shown.

We have previously shown that MHD patients demonstrated an anabolic resistance of muscle protein synthesis rates after mixed meal ingestion, supporting the notion that MHD patients may present with dysregulation in amino acid flux and metabolism (van Vliet *et al.* 2018). The findings from the present study suggest that this dysregulation in amino acid metabolism may be partly attributed to disruptions to the integrin-associate protein nexus in skeletal muscle. A decrease in the integrin-associated proteins may be explained by a separate finding that MHD patients display both increased basal myofibrillar protein synthesis and muscle caspase-3 protein content (van Vliet *et al.* 2018). This evidence, together with increased basal muscle protein synthesis and degradation rates, may indicate that MHD muscle is over-stimulated and remains in a state of constant flux (van Vliet *et al.* 2018). However, it is not clear why phenylalanine flux is reduced in MHD patients given that amino acid requirements are probably increased, given the raised muscle protein synthesis and breakdown rates in this population. However, this raised turnover may be linked to an up-regulation in the genes regulating the ubiquitin proteasome pathway (Hasselgren, 1999; Lecker *et al.* 1999; Mitch *et al.* 1999; Bodine *et al.* 2001; Ikemoto *et al.* 2001; St-Amand *et al.* 2001; Bey *et al.* 2003; Stevenson *et al.* 2003; Urso *et al.* 2006). In addition, the reduction in phenylalanine flux post meal, and thus the proposed availability to cell demands, may partly explain why this population group presents with both reduced muscle mass (van Vliet *et al.* 2018) and muscle atrophy (Johansen *et al.* 2003). Interestingly, van Vliet *et al.* (2018) also showed that both basal and fed-state muscle LAT1 protein content are decreased in MHD patients. LAT1 is an amino acid transporter found in proximity of capillaries (Hodson *et al.* 2018; van Vliet *et al.* 2018). Blood flow and capillary recruitment play a fundamental role in nutrient and hormonal delivery to muscle (Mitch *et al.* 1999; Williams *et al.* 2015). Therefore, a decrease in this protein in MHD could be a result of capillarity rarefaction in MHD skeletal muscles, which is linked to insulin resistance and poor nutrients perfusion (Mitch *et al.* 1999; Solomon *et al.* 2011; Bonner *et al.* 2013; Williams *et al.* 2015), a finding that may also have contributed to the reduced phenylalanine flux observed in our MHD sample.

Several studies suggest a role of the IPP complex in muscle degeneration (Gheyara *et al.* 2007; Postel *et al.* 2008). Postel *et al.* (2008) showed that zebrafish unable to express ILK developed mechanical instability in skeletal muscle. In addition, ILK-KO mice displayed progressive muscular dystrophy, with ILK mutants showing displacement of FAK, dystrophin and $\alpha 7\beta 1$D-integrin subunits (Gheyara *et al.* 2007). These results are similar to those observed in mice and humans lacking $\alpha 7$-integrin subunit, suggesting that ILK may act as a cytoplasmic effector of $\alpha 7\beta 1$-integrin in the pathogenesis of muscle degeneration (Gheyara *et al.* 2007; Postel *et al.* 2008). The adapter protein PINCH1 is known to bind with ILK and locates to integrin-mediated adhesion sites (Li *et al.* 2005; Stanchi *et al.* 2009; Karaköse *et al.* 2015). Several studies suggest a crucial role of PINCH1 in promoting cell adhesion, ECM assembly, muscle attachment and Akt activity (Wu, 1999; Eke *et al.* 2010; Vakaloglou & Zervas, 2012). Genetic ablation of PINCH1 in skeletal muscle results in cell death at the embryonic stage in mice (Sakai *et al.* 2003; Li *et al.* 2005; Wickström *et al.* 2010). Moreover, the interaction between ILK and PINCH1 is necessary to prevent degradation of IPP complex (Fukuda *et al.* 2003; Li *et al.* 2005), suggesting that defects in one of these proteins lead to impairment of the associated kinases of the IPP complex, partly supported by our finding that showed significant reductions in the protein content of ILK and PINCH1 in MHD skeletal muscle.

The inositol hexakisphosphate (IP6) kinase1 (IP6K1) produces the diphosphoinositol pentakisphosphate, which competes with phosphatidylinositol (3,4,5)-trisphosphate with respect to binding the pleckstrin homology domain of Akt, preventing Akt translocation to the cell membrane and its phosphorylation by PDK1, leading to decreased muscle ISI (Naufahu *et al.* 2018). IP6K1 can therefore represent a negative feedback mechanism in the insulin-dependent Akt pathway, which has been shown to be increased in insulin resistant models, whereas Akt is reduced (Chakraborty *et al.* 2010; Naufahu *et al.* 2018).

We further hypothesized that disruptions to the integrin-actin cytoskeleton linkage, largely as a result of impairments in the Rho GTPase Rac1, would result in upstream dysregulation of integrin-associated protein and Akt signalling in skeletal muscle, showing a decrease in Akt activity and an increase in IP6K1 protein, which may then contribute to the reduced nutrient handling in MHD patients. By contrast, our results showed that Rac1, as well as Akt2 and IP6K1, were similar in MHD muscle compared to insulin resistant matched controls despite differences in ILK and PINCH1.

These finding give rise to two notions (i) Rac1 and Akt2 probably do not play a major role in the development of insulin resistance in MHD muscle, given that MHD and controls present with similar levels of insulin resistance and muscle protein content of Rac1 and Akt2 and (ii) Rac1 is not essential for upstream integrin-associated protein regulation. In a separate experiment, we used a Rac1 KO rodent model to further investigate the role of this molecule on the integrin-associated protein signalling. These experiments revealed that there was no difference in the IPP complex protein content in Rac1 mKO compared to wild-type rodents. Both Rac1 and Akt are important regulators of insulin-stimulated glucose transport (JeBailey *et al.* 2007; Ueda *et al.* 2010; *Sylow et al. 2013a*, 2014; Moller *et al.* 2019). Several

studies suggest that Akt2 and Rac1 bifurcate downstream of phosphoinositide 3-kinase (Nozaki *et al.* 2012; Satoh, 2014; Takenaka *et al.* 2015) into two distinct parallel pathways, both promoting GLUT4 trafficking and muscle glucose uptake in an insulin-dependent manner (JeBailey *et al.* 2007; Ueda *et al.* 2008, 2010; Sylow *et al.* 2014; Raun *et al.* 2018; Moller *et al.* 2019), which is regulated via actin cytoskeleton organisation (Jaffe & Hall, 2005; Chiu *et al.* 2011; Sit & Manser, 2011; Spiering & Hodgson, 2011; Moller *et al.* 2019). Our data show that Rac1 is not different between MHD and non-MHD individuals and that both display similar degrees of ISI. In addition, our KO Rac1 mouse model showed no difference in integrin-associated proteins compared to the wild-type. Taken together, these data suggest that Rac1 may not be required for effective actin-integrin structural stability/remodelling or nutrient flux in MHD skeletal muscle. However, we cannot completely rule out a contribution of Rac1 in these processes. We recognize that whole-body phenylalanine kinetics and ISI are not direct measures of local amino acid turnover or insulin action in skeletal muscle, yet it has been recognized that skeletal muscle is a major disposal site for amino acids (Chang & Goldberg, 1978) and glucose (Thiebaud *et al.* 1982) in the postprandial state. We do acknowledge the limitations of our measurement and admit that the inclusion of multiple amino acid tracers and two-compartment models of glucose metabolism and ISI would offer a more accurate measures nutrient kinetics in this population. We also acknowledge that we analysed small sample size groups; therefore, further research involving more participants is required to give more robustness to our findings.

Conclusions

In conclusion, our results suggest that neither ISI, nor DI appear to be different between MHD patients and controls in the postprandial state. This finding may be explained by the similar levels of Rac1 and Atk2, two protein kinases implicated in insulin-dependent glucose uptake. Phenylalanine metabolism was lower within the MHD group, which may be linked to disruptions to the ILK-PINCH1 nexus and LAT1 (van Vliet *et al.* 2018), suggesting, for the first time, that the integrin-associated protein network may be required for effective nutrient uptake in skeletal muscle.

References

Bailey JL, Zheng B, Hu Z, Price SR & Mitch WE (2006). Chronic kidney disease causes defects in signaling through the insulin receptor substrate/phosphatidylinositol 3-kinase/Akt pathway: implications for muscle atrophy. *J Am Soc Nephrol* **17**, 1388–1394.

Barclay RD, Beals JW, Drnevich J, Imai BS, Yau PM, Ulanov AV, Tillin NA, Villegas-Montes M, Paluska SA, Watt PW, De Lisio M, Burd NA & Mackenzie RW (2020). Ingestion of lean meat elevates muscle inositol hexakisphosphate kinase 1 protein content independent of a distinct post-prandial circulating proteome in young adults with obesity. *Metabolism* **102**, 153996.

Bates D, Mächler M, Bolker BM & Walker SC (2015). Fitting linear mixed-effects models using lme4. *J Stat Softw* **67**, doi: https://doi.org/10.18637/jss.v067.i01.

Bergman EN, Reulein SS & Corlett RE (1989). Effects of obesity on insulin sensitivity and responsiveness in sheep. *Am J Physiol Endocrinol Metab* **257**, E772–E781.

Bey L, Akunuri N, Zhao P, Hoffman EP, Hamilton DG & Hamilton MT (2003). Patterns of global gene expression in rat skeletal muscle during unloading and low-intensity ambulatory activity. *Physiol Genomics* **13**, 157–167.

Bian Z-Q, Luo Y, Guo F, Huang Y-Z, Zhong M & Cao H (2019). Overexpressed ACP5 has prognostic value in colorectal cancer and promotes cell proliferation and tumorigenesis via FAK/PI3K/AKT signaling pathway. *Am J Cancer Res* **9**, 22–35.

Bisht B & Dey CS (2008). Focal adhesion kinase contributes to insulin-induced actin reorganization into a mesh harboring glucose transporter-4 in insulin resistant skeletal muscle cells. *BMC Cell Biol* **9**, 1–12.

Bisht B, Goel HL & Dey CS (2007). Focal adhesion kinase regulates insulin resistance in skeletal muscle. *Diabetologia* **50**, 1058–1069.

Bodine SC, Latres E, Baumhueter S, Lai VKM, Nunez L, Clarke BA, Poueymirou WT, Panaro FJ, Erqian Na, Dharmarajan K, Pan ZQ, Valenzuela DM, Dechiara TM, Stitt TN, Yancopoulos GD & Glass DJ (2001). Identification of ubiquitin ligases required for skeletal muscle atrophy. *Science* **294**, 1704–1708.

Bonner JS, Lantier L, Hasenour CM, James FD, Bracy DP & Wasserman DH (2013). Muscle-specific vascular endothelial growth factor deletion induces muscle capillary rarefaction creating muscle insulin resistance. *Diabetes* **62**, 572–580.

Burridge K & Wennerberg K (2004). Rho and Rac Take center stage. *Cell* **116**, 167–179.

Byun HJ, Lee JH, Kim BR, Kang S, Dong SM, Park MS, Lee SH, Park SH & Rho SB (2012). Anti-angiogenic effects of thioridazine involving the FAK-mTOR pathway. *Microvasc Res* **84**, 227–234.

Chakraborty A, Koldobskiy MA, Bello NT, Maxwell M, Potter JJ, Juluri KR, Maag D, Kim S, Huang AS, Dailey MJ, Saleh M, Snowman AM, Moran TH, Mezey E & Snyder SH (2010). Inositol pyrophosphates inhibit akt signaling, thereby regulating insulin sensitivity and weight gain. *Cell* **143**, 897–910.

Chambers MA, Moylan JS, Smith JD, Goodyear LJ & Reid MB (2009). Stretch-stimulated glucose uptake in skeletal muscle is mediated by reactive oxygen species and p38 MAP-kinase. *J Physiol* **587**, 3363–3373.

Chang TW & Goldberg AL (1978). The metabolic fates of amino acids and the formation of glutamine in skeletal muscle. *J Biol Chem* **253**, 3685–3693.

Chiu TT, Jensen TE, Sylow L, Richter EA & Klip A (2011). Rac1 signalling towards GLUT4/glucose uptake in skeletal muscle. *Cell Signal* **23**, 1546–1554.

Clemente CFMZ, Xavier-Neto J, Dalla Costa AP, Consonni SR, Antunes JE, Rocco SA, Pereira MB, Judice CC, Strauss B, Joazeiro PP, Matos-Souza JR & Franchini KG (2012). Focal adhesion kinase governs cardiac concentric hypertrophic growth by activating the AKT and mTOR pathways. *J Mol Cell Cardiol* **52**, 493–501.

DeFronzo RA, Jacot E, Jequier E, Maeder E, Wahren J & Felber JP (1981). The effect of insulin on the disposal of intravenous glucose. Results from indirect calorimetry and hepatic and femoral venous catheterization. *Diabetes* **30**, 1000–1007.

Deshmukh AS (2016). Insulin-stimulated glucose uptake in healthy and insulin-resistant skeletal muscle. *Horm Mol Biol Clin Investig* **26**, 13–24.

Eke I, Koch U, Hehlgans S, Sandfort V, Stanchi F, Zips D, Baumann M, Shevchenko A, Pilarsky C, Haase M, Baretton GB, Calleja V, Larijani B, Fässler R & Cordes N (2010). PINCH1 regulates Akt1 activation and enhances radioresistance by inhibiting PP1α. *J Clin Invest* **120**, 2516–2527.

Fukuda T, Chen K, Shi X & Wu C (2003). PINCH-1 is an obligate partner of integrin-linked kinase (ILK) functioning in cell shape modulation, motility, and survival. *J Biol Chem* **278**, 51324–51333.

Gastaldelli A, Coggan AR & Wolfe RR (1999). Assessment of methods for improving tracer estimation of non-steady-state rate of appearance. *J Appl Physiol* **87**, 1813–1822.

Gheyara AL, Vallejo-Illarramendi A, Zang K, Mei L, St-Amaud R, Dedhar S & Reichardt LF (2007). Deletion of integrin-linked kinase from skeletal muscles of mice resembles muscular dystrophy due to $\alpha 7\beta 1$-integrin deficiency. *Am J Pathol* **171**, 1966–1977.

Hasselgren PO (1999). Role of the ubiquitin-proteasome pathway in sepsis-induced muscle catabolism. *Mol Biol Rep* **26**, 71–76.

Hodson N, Brown T, Joanisse S, Aguirre N, West DWD, Moore DR, Baar K, Breen L & Philp A (2018). Characterisation of L-type amino acid transporter 1 (LAT1) expression in human skeletal muscle by immunofluorescent microscopy. *Nutrients* **10**, 23.

Huang D, Khoe M, Ilic D & Bryer-Ash M (2006). Reduced expression of focal adhesion kinase disrupts insulin action in skeletal muscle cells. *Endocrinology* **147**, 3333–3343.

Hynes RO (2002). Integrins: bidirectional, allosteric signaling machines. *Cell* **110**, 673–687.

Ikemoto M, Nikawa T, Takeda S, Watanabe C, Kitano T, Baldwin KM, Izumi R, Nonaka I, Towatari T, Teshima S, Rokutan K & Kishi K (2001). Space shuttle flight (STS-90) enhances degradation of rat myosin heavy chain in association with activation of ubiquitin-proteasome pathway. *FASEB J* **15**, 1279–1281.

Jaffe AB & Hall A (2005). RHO GTPASES: biochemistry and biology. *Annu Rev Cell Dev Biol* **21**, 247–269.

Jansson PA (2007). Endothelial dysfunction in insulin resistance and type 2 diabetes. *J Intern Med* **262**, 173–183.

JeBailey L, Wanono O, Niu W, Roessler J, Rudich A & Klip A (2007). Ceramide- and oxidant-induced insulin resistance involve loss of insulin-dependent Rac-activation and actin remodeling in muscle cells. *Diabetes* **56**, 394–403.

Jelinkova S, Fojtik P, Kohutova A, Vilotic A, Marková L, Pesl M, Jurakova T, Kruta M, Vrbsky J, Gaillyova R, Valášková I, Frák I, Lacampagne A, Forte G, Dvorak P, Meli AC & Rotrekl V (2019). Dystrophin deficiency leads to genomic instability in human pluripotent stem cells via no synthase-induced oxidative stress. *Cells* **8**, 53.

Jensen TE, Sylow L, Rose AJ, Madsen AB, Angin Y, Maarbjerg SJ & Richter EA (2014). Contraction-stimulated glucose transport in muscle is controlled by AMPK and mechanical stress but not sarcoplasmatic reticulum Ca^{2+} release. *Mol Metab* **3**, 742–753.

Johansen KL, Shubert T, Doyle J, Soher B, Sakkas GK & Kent-Braun JA (2003). Muscle atrophy in patients receiving hemodialysis: effects on muscle strength, muscle quality, and physical function. *Kidney Int* **63**, 291–297.

Kang L, Ayala JE, Lee-Young RS, Zhang Z, James FD, Neufer PD, Pozzi A, Zutter MM & Wasserman DH (2011). Diet-induced muscle insulin resistance is associated with extracellular matrix remodeling and interaction with integrin $\alpha 2\beta$ 1in mice. *Diabetes* **60**, 416–426.

Kang L, Lantier L, Kennedy A, Bonner JS, Mayes WH, Bracy DP, Bookbinder LH, Hasty AH, Thompson CB & Wasserman DH (2013). Hyaluronan accumulates with high-fat feeding and contributes to insulin resistance. *Diabetes* **62**, 1888–1896.

Kang L, Mayes WH, James FD, Bracy DP & Wasserman DH (2014). Matrix metalloproteinase 9 opposes diet-induced muscle insulin resistance in mice. *Diabetologia* **57**, 603–613.

Kang L, Mokshagundam S, Reuter B, Lark DS, Sneddon CC, Hennayake C, Williams AS, Bracy DP, James FD, Pozzi A, Zent R & Wasserman DH (2016). Integrin-linked kinase in muscle is necessary for the development of insulin resistance in diet-induced obese mice. *Diabetes* **65**, 1590–1600.

Karaköse E, Geiger T, Flynn K, Lorenz-Baath K, Zent R, Mann M & Fässler R (2015). The focal adhesion protein PINCH-1 associates with EPLIN at integrin adhesion sites. *J Cell Sci* **128**, 1023–1033.

Karusheva Y, Koessler T, Strassburger K, Markgraf D, Mastrototaro L, Jelenik T, Simon MC, Pesta D, Zaharia OP, Bódis K, Bärenz F, Schmoll D, Wolkersdorfer M, Tura A, Pacini G, Burkart V, Müssig K, Szendroedi J & Roden M (2019). Short-term dietary reduction of branched-chain amino acids reduces meal-induced insulin secretion and modifies microbiome composition in type 2 diabetes: a randomized controlled crossover trial. *Am J Clin Nutr* **110**, 1098–1107.

Kobayashi S, Maesato K, Moriya H, Ohtake T & Ikeda T (2005). Insulin resistance in patients with chronic kidney disease. *Am J Kidney Dis* **45**, 275–280.

Kramer HF, Witczak CA, Fujii N, Jessen N, Taylor EB, Arnolds DE, Sakamoto K, Hirshman MF & Goodyear LJ (2006). Distinct signals regulate AS160 phosphorylation in response to insulin, AICAR, and contraction in mouse skeletal muscle. *Diabetes* **55**, 2067–2076.

Lecker SH, Solomon V, Mitch WE & Goldberg AL (1999). Clinical trials for the treatment of secondary wasting and cachexia muscle protein breakdown and the critical role of the ubiquitin- proteasome pathway in normal and disease states 1, 2. *J Nutr* **129**, 227S-237S.

Legate KR & Fässler R (2009). Mechanisms that regulate adaptor binding to β-integrin cytoplasmic tails. *J Cell Sci* **122**, 187–198.

Li S, Bordoy R, Stanchi F, Moser M, Braun A, Kudlacek O, Wewer UM, Yurchenco PD & Fässler R (2005). PINCH1 regulates cell-matrix and cell-cell adhesions, cell polarity and cell survival during the peri-implantation stage. *J Cell Sci* **118**, 2913–2921.

Lorenzo C, Hanley AJG, Wagenknecht LE, Rewers MJ, Stefanovski D, Goodarzi MO & Haffner SM (2013). Relationship of insulin sensitivity, insulin secretion, and adiposity with insulin clearance in amultiethnic population: the insulin resistance atherosclerosis study. *Diabetes Care* **36**, 101–103.

Mackenzie RWA & Elliott BT (2014). Akt/PKB activation and insulin signaling: a novel insulin signaling pathway in the treatment of type 2 diabetes. *Diabetes Metab Syndr Obes* **7**, 55–64.

Von der Mark H, Durr J, Sonnenberg A, Von der Mark K, Deutzmann R & Goodman SL (1991). Skeletal myoblasts utilize a novel β1-series integrin and not $\alpha6\beta1$ for binding to the E8 and T8 fragments of laminin. *J Biol Chem* **266**, 23593–23601.

Matsuda M & Defronzo RA (1999). Insulin sensitivity indices obtained from comparison with the euglycemic insulin clamp. *Diabetes Care* **22**, 1462–1470.

Matthews DE (2007). An overview of phenylalanine and tyrosine kinetics in humans. *J Nutr* **137**, 1549S–1555S.

Mayer U, Saher G, Fässler R, Bornemann A, Echtermeyer F, von der Mark H, Miosge N, Posch E & von der Mark K (1997). Absence of integrin α7 causes a novel form of muscular dystrophy. *Nat Genet* **15**, 57–61.

Mitch WE, Bailey JL, Wang X, Jurkovitz C, Newby D & Russ Price S (1999). Evaluation of signals activating ubiquitin-proteasome proteolysis in a model of muscle wasting. *Am J Physiol Cell Physiol* **276**, C1132–C1138.

Moller LLV, Klip A & Sylow L (2019). Rho GTPases-emerging regulators of glucose homeostasis and metabolic health. *Cells* **8**, 434.

Naufahu J, Elliott B, Markiv A, Dunning-Foreman P, McGrady M, Howard D, Watt P & MacKenzie RWA (2018). High-intensity exercise decreases IP6K1 muscle content and improves insulin sensitivity (S i 2 $*$) in glucose-intolerant individuals. *J Clin Endocrinol Metab* **103**, 1479–1490.

Nozaki S, Ueda S, Takenaka N, Kataoka T & Satoh T (2012). Role of RalA downstream of Rac1 in insulin-dependent glucose uptake in muscle cells. *Cell Signal* **24**, 2111–2117.

Pattison JS, Folk LC, Madsen RW, Childs TE & Booth FW (2004). Transcriptional profiling identifies extensive downregulation of extracellular matrix gene expression in sarcopenic rat soleus muscle. *Physiol Genomics* **15**, 34–43.

Peter AK, Cheng H, Ross RS, Knowlton KU & Chen J (2011). The costamere bridges sarcomeres to the sarcolemma in striated muscle. *Prog Pediatr Cardiol* **31**, 83–88.

Postel R, Vakeel P, Topczewski J, Knöll R & Bakkers J (2008). Zebrafish integrin-linked kinase is required in skeletal muscles for strengthening the integrin-ECM adhesion complex. *Dev Biol* **318**, 92–101.

Raun SH, Ali M, Kjøbsted R, Møller LLV, Federspiel MA, Richter EA, Jensen TE & Sylow L (2018). Rac1 muscle knockout exacerbates the detrimental effect of high-fat diet on insulin-stimulated muscle glucose uptake independently of Akt. *J Physiol* **596**, 2283–2299.

Sakai T, Li S, Docheva D, Grashoff C, Sakai K, Kostka G, Braun A, Pfeifer A, Yurchenco PD & Fässler R (2003). Integrin-linked kinase (ILK) is required for polarizing the epiblast, cell adhesion, and controlling actin accumulation. *Genes Dev* **17**, 926–940.

Satoh T (2014). Molecular mechanisms for the regulation of insulin-stimulated glucose uptake by small guanosine triphosphatases in skeletal muscle and adipocytes. *Int J Mol Sci* **15**, 18677–18692.

Semenkovich CF (2006). Review series Insulin resistance and atherosclerosis. *J Clin Invest* **116**, 1813–1822.

Sit ST & Manser E (2011). Rho GTPases and their role in organizing the actin cytoskeleton. *J Cell Sci* **124**, 679–683.

Solomon TPJ, Haus JM, Li Y & Kirwan JP (2011). Progressive hyperglycemia across the glucose tolerance continuum in older obese adults is related to skeletal muscle capillarization and nitric oxide bioavailability. *J Clin Endocrinol Metab* **96**, 1377–1384.

Spiering D & Hodgson L (2011). Dynamics of the rho-family small GTPases in actin regulation and motility. *Cell Adhes Migr* **5**, 170–180.

St-Amand J, Okamura K, Matsumoto K, Shimizu S & Sogawa Y (2001). Characterization of control and immobilized skeletal muscle: an overview from genetic engineering. *FASEB J* **15**, 684–692.

Stanchi F, Grashoff C, Yonga CFN, Grall D, Fässler R & Van Obberghen-Schilling E (2009). Molecular dissection of the ILK-PINCH-parvin triad reveals a fundamental role for the ILK kinase domain in the late stages of focal-adhesion maturation. *J Cell Sci* **122**, 1800–1811.

Stevenson EJ, Giresi PG, Koncarevic A & Kandarian SC (2003). Global analysis of gene expression patterns during disuse atrophy in rat skeletal muscle. *J Physiol* **551**, 33–48.

Sylow L, Jensen TE, Kleinert M, Højlund K, Kiens B, Wojtaszewski J, Prats C, Schjerling P & Richter EA (2013*a*). Rac1 signaling is required for insulin-stimulated glucose uptake and is dysregulated in insulin-resistant murine and human skeletal muscle. *Diabetes* **62**, 1865–1875.

Sylow L, Jensen TE, Kleinert M, Mouatt JR, Maarbjerg SJ, Jeppesen J, Prats C, Chiu TT, Boguslavsky S, Klip A, Schjerling P & Richter EA (2013*b*). Rac1 is a novel regulator of contraction-stimulated glucose uptake in skeletal muscle. *Diabetes* **62**, 1139–1151.

Sylow L, Kleinert M, Pehmøller C, Prats C, Chiu TT, Klip A, Richter EA & Jensen TE (2014). Akt and Rac1 signaling are jointly required for insulin-stimulated glucose uptake in skeletal muscle and downregulated in insulin resistance. *Cell Signal* **26**, 323–331.

Sylow L, Kleinert M, Richter EA & Jensen TE (2017). Exercise-stimulated glucose uptake-regulation and implications for glycaemic control. *Nat Rev Endocrinol* **13**, 133–148.

Sylow L, Møller LLV, Kleinert M, Richter EA & Jensen TE (2015). Stretch-stimulated glucose transport in skeletal muscle is regulated by Rac1. *J Physiol* **593**, 645–656.

Takenaka N, Nihata Y & Satoh T (2015). Immunofluorescent detection of the activation of the small GTPase Rac1 in mouse skeletal muscle fibers. *Anal Biochem* **476**, 5–7.

Tang CH, Lu DY, Tan TW, Fu WM & Yang R Sen (2007). Ultrasound induces hypoxia-inducible factor-1 activation and inducible nitric-oxide synthase expression through the integrin/integrin-linked kinase/Akt/mammalian target of rapamycin pathway in osteoblasts. *J Biol Chem* **282**, 25406–25415.

Thiebaud D, Jacot E, DeFronzo RA, Maeder E, Jequier E & Felber JP (1982). The effect of graded doses of insulin on total glucose uptake, glucose oxidation, and glucose storage in man. *Diabetes* **31**, 957–963.

Thomas SS, Zhang L & Mitch WE (2015). Molecular mechanisms of insulin resistance in chronic kidney disease. *Kidney Int* **88**, 1233–1239.

Török D, Patel N, JeBailey L, Thong FSL, Randhawa VK, Klip A & Rudich A (2004). Insulin but not PDGF relies on actin remodeling and on VAMP2 for GLUT4 translocation in myoblasts. *J Cell Sci* **117**, 5447–5455.

Tuguzbaeva G, Yue E, Chen X, He L, Li X, Ju J, Qin Y, Pavlov V, Lu Y, Jia W, Bai Y, Niu Y & Yang B (2019). PEP06 polypeptide 30 is a novel cluster-dissociating agent inhibiting αv integrin/FAK/Src signaling in oral squamous cell carcinoma cells. *Acta Pharm Sin B* **9**, 1163–1173.

Turcotte LP & Fisher JS (2008). Skeletal muscle insulin resistance: roles of fatty acid metabolism and exercise. *Phys Ther* **88**, 1279–1296.

Ueda S, Kataoka T & Satoh T (2008). Activation of the small GTPase Rac1 by a specific guanine-nucleotide-exchange factor suffices to induce glucose uptake into skeletal-muscle cells. *Biol Cell* **100**, 645–661.

Ueda S, Kitazawa S, Ishida K, Nishikawa Y, Matsui M, Matsumoto H, Aoki T, Nozaki S, Takeda T, Tamori Y, Aiba A, Kahn CR, Kataoka T & Satoh T (2010). Crucial role of the small GTPase Rac1 in insulin-stimulated translocation of glucose transporter 4 to the mouse skeletal muscle sarcolemma. *FASEB J* **24**, 2254–2261.

Urso ML, Scrimgeour AG, Chen YW, Thompson PD & Clarkson PM (2006). Analysis of human skeletal muscle after 48 h immobilization reveals alterations in mRNA and protein for extracellular matrix components. *J Appl Physiol* **101**, 1136–1148.

Utzschneider KM, Prigeon RL, Faulenbach MV, Tong J, Carr DB, Boyko EJ, Leonetti DL, McNeely MJ, Fujimoto WY & Kahn SE (2009). Oral disposition index predicts the development of future diabetes above and beyond fasting and 2-h glucose levels. *Diabetes Care* **32**, 335–341.

Uwaifo GI, Fallon EM, Chin J, Elberg J, Parikh SJ & Yanovski JA (2002). Indices of insulin action, disposal, and secretion derived from fasting samples and clamps in normal glucose-tolerant black and white children. *Diabetes Care* **25**, 2081 LP–2087.

Vakaloglou K & Zervas C (2012). Parvin-ILK. *Bioarchitecture* **2**, 91–94.

van Vliet S, Beals JW, Parel JT, Hanna CD, Utterback PL, Dilger AC, Ulanov AV, Li Z, Paluska SA, Moore DR, Parsons CM & Burd NA (2016). Development of intrinsically labeled eggs and poultry meat for use in human metabolic research. *J Nutr* **146**, 1428–1433.

van Vliet S, Skinner SK, Beals JW, Pagni BA, Fang HY, Ulanov AV, Li Z, Paluska SA, Mazzulla M, West DWD, Moore DR, Wilund KR & Burd NA (2018). Dysregulated handling of dietary protein and muscle protein synthesis after mixed-meal ingestion in maintenance hemodialysis patients. *Kidney Int Reports* **3**, 1403–1415.

Wang HV, Chang LW, Brixius K, Wickström SA, Montanez E, Thievessen I, Schwander M, Müller U, Bloch W, Mayer U & Fässler R (2008). Integrin-linked kinase stabilizes myotendinous junctions and protects muscle from stress-induced damage. *J Cell Biol* **180**, 1037–1049.

Welinder C & Ekblad L (2011). Coomassie staining as loading control in western blot analysis. *J Proteome Res* **10**, 1416–1419.

Wickström SA, Lange A, Montanez E & Fässler R (2010). The ILK/PINCH/parvin complex: the kinase is dead, long live the pseudokinase! *EMBO J* **29**, 281–291.

Williams AS, Kang L & Wasserman DH (2015). The extracellular matrix and insulin resistance. *Trends Endocrinol Metab* **26**, 357–366.

Workeneh BT & Mitch WE (2010). Review of muscle wasting associated with chronic kidney disease. *Am J Clin Nutr* **91**, 1128S-1132S.

Wright DC, Geiger PC, Holloszy JO & Han DH (2005). Contraction- and hypoxia-stimulated glucose transport is mediated by a Ca^{2+}-dependent mechanism in slow-twitch rat soleus muscle. *Am J Physiol Endocrinol Metab* **288**, E1062–E1066.

Wu C (1999). Integrin-linked kinase and PINCH: partners in regulation of cell-extracellular matrix interaction and signal transduction. *J Cell Sci* **112**, 4485–4489.

Wu C & Dedhar S (2001). Integrin-linked kinase (ILK) and its interactors: a new paradigm for the coupling of extracellular matrix to actin cytoskeleton and signaling complexes. *J Cell Biol* **155**, 505–510.

Additional information

Data availability statement

The data that support the findings of this study are openly available in figshare at: https://doi.org/10.6084/m9.figshare.12886943.

Competing interests

The authors declare that they have no competing interests.

Author contributions

FD, RM and LS contributed to the conception and design of the experiment. FD and RM contributed to the analysis and

interpretation of data. RM, OA, KRW, SVV, PW, DR and NAB contributed to drafting the article or revising it with respect to intellectual content. FD and RM had primary responsibility for the final content. Each author contributed important intellectual content during the drafting or revision of the article, accepts personal accountability for the author's own contributions, and agrees to ensure that questions pertaining to the accuracy or integrity of any portion of the work are appropriately investigated and resolved.

Funding

This research did not receive any specific grant from funding agencies in the public, commercial or not-for-profit sectors.

Acknowledgements

We sincerely thank Dr Lykke Sylow and Professor Erik A. Ritcher of the Department of Nutrition, Exercise and Sport, University of Copenhagen, who have supported this project and shared their materials and facilities for the experiments. Our personal thanks are extended to Mona Sadek-Ali from Dr Sylow's laboratory for her constant help and support. Moreover, we thank Dr Nicholas A. Burd and his group from the University of Illinois for sharing their materials for this project.

Keywords

cytoskeleton, haemodialysis, ILK, insulin, integrins, metabolism, phenylalanine, PINCH, Rac1

Supporting information

Additional supporting information may be found online in the Supporting Information section at the end of the article.

Statistical Summary Document